Expansion of an ablation plume in a buffer gas and cluster growth

To cite this article: A. Bailini and P. M. Ossi 2007 *EPL* **79** 35002

A Letters Journal Exploring the Frontiers of Physics

August 2007

EPL, **79** (2007) 35002
doi: 10.1209/0295-5075/79/35002

www.epljournal.org

Expansion of an ablation plume in a buffer gas and cluster growth

A. Bailini and P. M. Ossi[(a)]

Dipartimento di Ingegneria Nucleare, Centre of Excellence "Nano Engineered MAterials and Surfaces - NEMAS", Politecnico di Milano - Via Ponzio 34-3, 20133, Milano, Italy

received 14 March 2007; accepted in final form 20 June 2007
published online 20 July 2007

PACS 52.38.Mf – Laser ablation
PACS 82.33.Xj – Plasma reactions (including flowing afterglow and electric discharges)
PACS 81.07.-b – Nanoscale materials and structures: fabrication and characterization

Abstract – The mixed propagation model is introduced to describe the expansion through a buffer gas of the plasma produced by pulsed-laser ablation. After testing the model against the results of representative experiments, the deduced expansion parameter values are used to model the growth of clusters that are nucleated in the plume. For plumes of silicon and tungsten propagating in helium as well as of tantalum propagating in oxygen cluster size is evaluated and compared (silicon; tungsten) with experimental data.

Introduction. – A peculiar feature of nanostructured materials is the dramatic dependence of several relevant physical properties on the size of the constituent particles. The latter are found in a variety of laboratory and natural plasmas [1–3] and are both interesting from the fundamental point of view and promising for several technological applications. When clusters are the constituents of a nanostructured solid the number of atoms per cluster, ranging from a few to several tens of thousands atoms causes strong variations of the surface-to-bulk atom ratio. A careful size control of the constituent clusters is a challenging step [4], preliminary to any tailoring of the structure and morphology of a cluster-assembled (CA) film.

In pulsed-laser deposition (PLD) the energetic species ablated from the surface of a solid target constitute a micro-plasma called plume. During the target-to-substrate flight plume characteristics, including the number densities of atoms and clusters, the fraction of ionised species, their charge state, the number densities of electrons and neutrals change and define plume energetics, expansion and interaction with the surroundings. In particular, when PLD using nanosecond pulses is performed in a buffer gas [5] films spanning wide density and porosity intervals, from compact, with density approaching the theoretical one, to highly porous are produced. With respect to vacuum, in a plume propagating through a gas the observed fluorescence is stronger due to particle collisions both in the plume expansion front and in the body, the plume edge is better defined as a result of the presence of a shock wave front, the plume is spatially confined, its internal pressure progressively reduces, the shock wave front slows down and fast species in the shock front are reached by slow constituents. In the shock region the temperature raises up to several thousands of kelvin degrees and enhanced optical emission from excited species in the plasma is observed. In turn, plume confinement results in a lowering of the cooling rate of the plume. Under such conditions mutual aggregation of plume constituents occurs. The basic questions are where, when, *i.e.* on what time scale and how, *i.e.* by what mechanism(s) do condensate the nanoparticles observed at the surface of a substrate when deposition is interrupted after a small number of laser pulses. Answering to these questions allows to solve the still open problem of nanocluster growth in a buffer gas and to optimise the rate of cluster formation. The present work moves in this direction. A further problem inherent to a complete control of film growth is how do clusters aggregate and possibly coalesce, depending on the deposition time and the nature, morphology and temperature of the substrate where they land and diffuse. Focusing our attention on plume behaviour, experiments showed three different regimes [6], extending over well-defined ranges of buffer gas pressure, of energy of plasma constituents and of propagation time. They are an initial "vacuum-like" stage with forward-directed flow and weak scattering of the ablated products, followed by a transition stage with strong momentum transfer to the buffer gas and weak scattering of the ablated species and finally a diffusion regime at high pressure. In the latter stage plume constituents

[(a)]E-mail: paolo.ossi@polimi.it

form a confined, sphere-like structure [7]. Buffer gas affects the spatial distribution, deposition rate, kinetic energy and kinetic energy distribution of plume constituents [8], thus influencing cluster formation and evolution, as well as cluster energy distribution in the plume. Deviations from free expansion of the plume occur when the mass of snowploughed buffer gas at the plume periphery becomes comparable with plume mass M_p. The radius r_p of the hemispherical plume is given by

$$r_p = [(3M_p k_B T_g)/(2\pi m_g)]^{1/3}\ p_g^{-1/3}, \qquad (1)$$

where k_B is the Boltzmann constant and T_g, m_g, p_g are the temperature, atomic mass and pressure of the buffer gas [6].

Given the characteristics of plume expansion, it is unrealistic to search for a single model able to completely describe the observed phenomena and every analytical model is adequate to represent a specific expansion stage. In particular, three analytical models, the *shock-wave* model [9,10], the *drag* model [9,11,12] and the *diffusion* model [13] have been introduced and were recently discussed [14]. The shock wave model, particularly in the delayed form [9], correctly fits experimental data at *large* values of time and buffer gas pressure. The drag model, again in its delayed version [9] provides good fits to the *early* expansion stage, but beyond a gas pressure around 10^2 Pa and time around $4\,\mu$s the plume velocity is overestimated. Moreover the plume is expected to stop at a distance $x_{st} \cong 4$–$5l$ from the target [15], with $l = (n_g\sigma)^{-1}$ the mean free path of the ablated species in the gas, σ being the pertinent scattering cross-section. Therefore, beyond a lower threshold, buffer gas pressure results in a non-linear dependence of the plasma front edge on the distance from the target. The classical diffusion model [13] considerably underestimates the distance travelled by the plume. The analytical phenomenological model developed by Arnold *et al.* [16] includes three different dependencies on time of the plume front position x, corresponding to different families of curves $x(t)$. The presentation of data on a single curve results from adopting dimensionless variables.

Besides analytical models, by gas-dynamic numerical approaches [17–19] good fits to specific experiments were obtained; yet the degree of complexity of the mathematical treatments and the required approximations limit their applicability.

All the models just introduced provide an *a posteriori interpretation* of experimental data, but they have *no* predictive capability about plume dynamics, given their dependence on purely numerical fitting parameters. In the following a two-stage analytical approach that accounts for plume expansion under rather general conditions is introduced and tested against experimental data on the propagation of ablation plumes in silicon, tantalum and tungsten. Model parameters have a clear physical meaning and depend on easily available process parameters such as buffer gas nature, pressure and temperature, number density of ablated species, target-substrate distance. This makes it possible to *predict* plume expansion for broad ranges of experiments in which a specific choice of process parameter values was fixed. The deduced values of the model parameters for plume propagation are then used to calculate the size of clusters growing in the plume. Model predictions are compared to available data on the size of clusters in CA silicon and tungsten films deposited by PLD.

Mixed propagation model. – The quasi-explosive initial plume expansion results in a Knudsen layer [20], where the leading contribution is the particle flux velocity. The particles ejected from the target surface have a strongly dominant velocity component in the direction normal to the surface. If we still retain a diffusive character of particle motion, this coincides with diffusion through a medium of correspondingly lowered effective density. The presence of Knudsen layer may be mimicked introducing a significantly reduced value for the *effective* number density of the buffer gas, n_{eff}. The non-Maxwellian velocity distribution affects also particle propagation beyond the Knudsen layer. Adopting n_{eff} the *modified diffusion* model results, with a diffusion coefficient [14,21]

$$D' = Klv_0 = Kv_0(n\sigma)^{-1}, \qquad (2)$$

where v_0 is the ejection velocity from the target of the *fastest* group of ablated particles in the plume front. Such an experimental parameter is obtained from the initial slope of the measured distance-time plot for plumes produced and propagating under given conditions. The choice of v_0 instead of the usual thermal velocity v of the particles is an ansatz of the model, whose meaning is to maximise the weight of flux velocity, considering the fastest particle group with the maximum flux velocity. Although the velocity of the plume front lowers during expansion (see figs. 1 and 2 below) the fit of the modified diffusion model to experimental data is good, particularly beyond the very initial plume expansion stage where plume velocity is overestimated. This implies that flux velocity indirectly influences in a meaningful way plume propagation also at comparatively *large* distances from the target.

Plume velocities measured during propagation through different gases, after UV laser irradiation of elemental targets including C, Si, Sn, Ag, Ta, W were analysed [22]. The K values providing better fits to the data scale with the atomic mass of the target, ranging from $K = 2$ (light elements: C; Si) to $K = 6$ (intermediate-mass elements: Ag; Sn) to $K = 8$ (heavy elements: Ta; W). Thus, given the target mass, the K value is uniquely defined. Notice that in the range of particle velocities of our concern the scattering cross-sections are essentially unknown, so that alternatively the usual diffusion coefficient D could be used together with smaller σ values.

To reproduce the experimentally observed initial linear behaviour of plume expansion (see, *e.g.*, [19] for Si and [12]

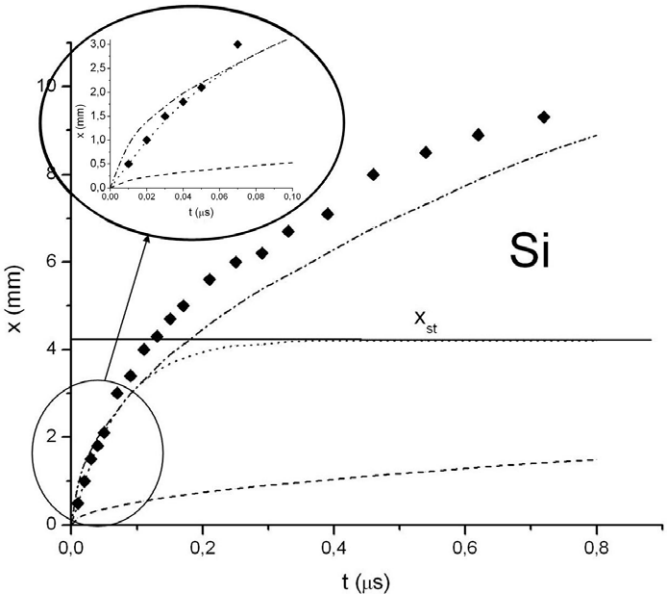

Fig. 1: Distance x (diamonds) travelled by propagating silicon [19] ablation plumes as a function of time. Dashed line: diffusion model; dash-dotted line: modified diffusion model; dotted line: modified drag model. The inset shows that modified drag model fits correctly the initial linear expansion of the plume.

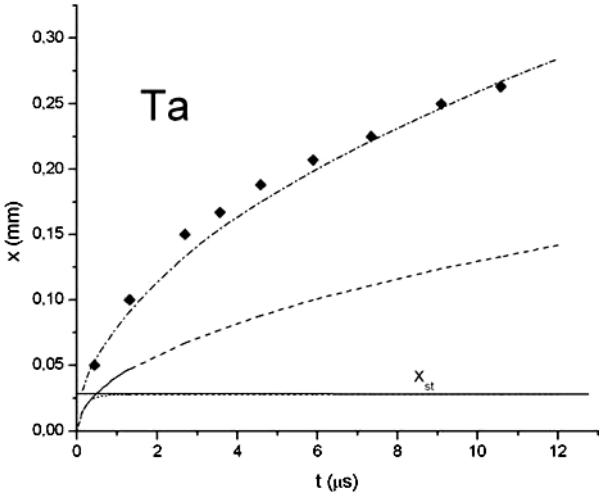

Fig. 2: Distance x (diamonds) travelled by propagating tantalum [24] ablation plumes as a function of time. General information as for fig. 1.

for C) only drag model is suitable. Now for simplicity the one-dimensional plume expansion along the principal plume axis x is considered. In the literature [9,11,12] the drag model is displayed in the form

$$x(t) = x_{st}\,[1 - \exp(-bt)], \tag{3}$$

where x_{st} and b are purely fitting parameters. Moving from the equation that describes the diffusion dynamics of a fluid of classical particles in the presence of viscosity, whose effect is embodied in a coefficient μ [23], with the initial conditions $x(0) = 0$ and $(\mathrm{d}x/\mathrm{d}t)(0) = v_0$, the position $x(t)$ of an atom is

$$x(t) = v_0 D' \mu^{-1}[1 - \exp(-\mu\, D'^{-1} t)]. \tag{4}$$

In such a *modified drag* model both the slowing down coefficient $b = \mu D'^{-1}$ and the stopping distance $x_{st} = v_0 D' \mu^{-1}$ take a clear physical meaning.

Experiments [6,8] show that initially the number density n_a of the ablated particles is larger than the buffer gas density n_g, but the rapid plume expansion leads to a density decrease down to $n_a = n_g$, when a stable shock wave front is formed and the expansion regime changes. At shock wave formation the inequality $n_a < n_g$ is established in the body of the plume. Gas atoms are strongly scattered by fast plume constituents (normally, positive ions) that are slowed down and aggregate themselves with the slower particles initially grouped in the plume body and tail.

The sequence of such complex phenomena is reflected by the combination of *modified* diffusion and *modified* drag models to give mixed-propagation model. In the model the distance x_{st} corresponds to an unphysical discontinuity of plume propagation and represents the region where the viscous slowing-down of the plume front leads to the formation of the stable shock wave front; at distances $x < x_{st}$ the modified drag model holds, while for $x \geqslant x_{st}$ the modified diffusion model holds. The x_{st} value is chosen according to the estimate $x_{st} \cong 4l$ [15] and it is calculated using the n_g and pertinent σ values.

According to the modified drag model the plume should stop after having travelled the short distance x_{st}, contrary to experiment. On the other hand, the modified diffusion model predicts propagation distances larger than the observed ones both in the early plume expansion stages and at low pressure of the buffer gas; the *mixed-propagation* model takes into account both the above limitations. Notice that at low ambient pressure (not higher than 1 Pa), the stopping distance x_{st} nearly coincides with usual values of the target-substrate distance $x_{T\text{-}S}$ (a few centimetres), so that the modified drag model is enough to describe plume dynamics. The mixed-propagation model has general applicability and *predictive ability* because the necessary input parameters are the highest escape velocity v_0 of ablated particles, the geometric scattering cross-sections σ, the number densities n_g of the gas, as obtained from gas pressure and n_a of the ablated particles, which is calculated from the number of particles ablated by a single pulse and from imaged average plume volume.

Plume propagation. – The mixed-propagation model is now tested against literature results on the propagation of plumes ablated from elemental targets of the light semiconductor Si [19] and of the heavy refractory metal Ta [24]. The first were originally analysed by the shock wave model and the latter by the drag model. Then, the expansion of W plumes is studied. In table 1 data are collected from ablation experiments on silicon in helium, tantalum in oxygen and tungsten in helium, at different gas pressures;

Table 1: Collection of data from silicon [19], tantalum [24] and tungsten [30] ablation experiments (upper part) and of mixed-propagation model parameters (lower part).

	λ(nm)	f(J cm^{-2})	τ(ns)	$x_{T\text{-}S}$(cm)	p_g(Pa)	n_g(cm^{-3})
Si	532	4.0	8	5	65	$1.6 \cdot 10^{16}$
Ta	532	5.0	6	3	20	$4.8 \cdot 10^{15}$
W_1	248	4.5	20	5	40	$9.7 \cdot 10^{15}$
W_2	248	4.5	20	5	60	$1.5 \cdot 10^{16}$
W_3	248	4.5	20	5	200	$4.8 \cdot 10^{16}$
	n_a(cm^{-3})	$\sigma_{g\text{-}a}$(cm^2)	$\sigma_{a\text{-}a}$(cm^2)	v(cm μs^{-1})	t_f(μs)	x_{aggr}(cm)
Si	$3 \cdot 10^{16}$	$7.5 \cdot 10^{-16}$	$2.2 \cdot 10^{-15}$	3.0	4.64	2.6
Ta	$5 \cdot 10^{15}$	$3.7 \cdot 10^{-15}$	$7.5 \cdot 10^{-15}$	0.7	0.68	3.3
W_1	$6.7 \cdot 10^{13}$	$1.04 \cdot 10^{-15}$	$3.2 \cdot 10^{-15}$	0.8	6.89	2.87
W_2	$2.4 \cdot 10^{14}$	$1.04 \cdot 10^{-15}$	$3.2 \cdot 10^{-15}$	0.8	8.79	2.65
W_3	$1.5 \cdot 10^{15}$	$1.04 \cdot 10^{-15}$	$3.2 \cdot 10^{-15}$	0.8	18.10	2.08

also parameter values used in mixed-propagation model are reported. In fig. 1 data [19] on the propagation of the front of silicon plumes in helium (diamonds) obtained by recording ICCD pictures of the plume self-emission are shown. Fits to the data with diffusion model (dashed line), modified diffusion model (dash-dotted line) and modified drag model (dotted line) are displayed. The latter well reproduces the linear trend of the first plume expansion stage, but it incorrectly predicts that plume is stopped at x_{st}. Diffusion model is evidently inaccurate; its modified version gives a reasonable fit to data at intermediate and delayed times, although it slightly overestimates propagation distances near the target. The value of v_0 used in the fit is 6 cm μs^{-1} [18]; taking $x_{st} = 4l$, $b = v_0(4l)^{-1}$ is obtained. For this element $K = 2$. Looking at fig. 1 the modified diffusion model reproduces all stages of plume expansion in an accurate enough way. The extent of accuracy is comparable to that of the original data analysis [19], yet, if *ad hoc* experiments were performed focusing on the very initial plume propagation, within 0.1 μs (see the inset of fig. 1), the linear behaviour predicted by modified drag model would be most suited.

Figure 2 shows the result of the application of diffusion (dashed line), modified diffusion (dash-dotted line) and modified drag model (dotted line) to ablation experiments on tantalum in oxygen [24], starting from optical emission spectroscopy data. The delayed peak of the emission profile recorded at a fixed distance from the target is studied; this peak appears also when Ta is ablated in argon. The peak is associated [24] to excitation of ablated TaO molecules and it represents the plume component *independent* of gas-phase chemical reactions, due to the particular buffer gas used. The trend of the fits is similar to that discussed for silicon. No data are available on the early plume expansion stage of Ta; experimental data fall beyond the stopping distance x_{st}, so that the modified diffusion model is sufficient to describe plume dynamics; the values of v_0 used in the fit is 1.5 cm μs^{-1} [24]. Again, the fit obtained by mixed-propagation model is of equivalent quality to that of the literature analysis [24]. Summarising, for both examined elements, the mixed-propagation model is of comparable accuracy to existing approaches, but it does not require using fitting parameters, apart from K, whose value must however be chosen among the three discussed above; besides this, the model is suitable for a wide range of ablation conditions.

In the case of tungsten $v_0 = 1.5$ cm μs^{-1} [25]; the datum refers to ablation experiments performed in vacuum, but v_0 value is independent of gas pressure [26]; plume velocity during expansion in the gas was not measured. Yet, given the strong similarity between Ta and W concerning density, hardness, melting and evaporation temperatures and heats [27] it is assumed that the expansion of W plumes is comparable to that of Ta plumes, as shown in fig. 2.

The results of mixed-propagation model are particularly useful as input parameters to model cluster growth in the expanding plume.

Cluster growth. – It is usually considered that cluster formation proceeds through the separate steps of nucleation, growth and cooling [28]. In all steps cluster evolution is affected mainly by the propagation dynamics of the plume. When a buffer gas is present, the control of cluster formation requires solving a set of hydrodynamic equations for plume expansion through the gas, while taking into account the dynamics of vapour condensation. This "exact" approach is out of the present calculation capabilities. To strongly simplify the problem, we exclude from the analysis the first stage, assuming that the plume propagates under conditions such that an initial seed population of tiny clusters is available [29]. Thus we assume that the mechanisms of cluster formation do not affect plume evolution [28]. The picture of plume expansion given by mixed-propagation model is used to find a simple expression for the average number N of

atoms in a cluster grown up to its equilibrium *maximum* size during plume flight. The plume experiences different internal pressure regimes and is spatially inhomogeneous, so that clusters in different regions of the plume evolve through the above steps at different times, yet averages over long times are considered here.

Under these hypotheses in the ideal gas approximation, N is given by

$$N = (n_a \cdot \sigma_{a\text{-}a} \cdot \langle v \rangle \cdot t_f) \cdot (n_g \cdot \sigma_{a\text{-}g} \cdot \langle v \rangle \cdot t_f) \cdot x_{T\text{-}S}\, x_{aggr}^{-1},$$
$$\text{for } x_{T\text{-}S} < x_{aggr} \tag{5a}$$

and by

$$N = (n_a \cdot \sigma_{a\text{-}a} \cdot \langle v \rangle \cdot t_f) \cdot (n_g \cdot \sigma_{a\text{-}g} \cdot \langle v \rangle \cdot t_f),$$
$$\text{for } x_{T\text{-}S} > x_{aggr}. \tag{5b}$$

In both equations x_{aggr} is the distance travelled by the plume until cluster growth continues. This is deduced by optical spectroscopy data, recording the signal from the relevant species (for example, TaO, in the case of Ta) in the plume as a function of the distance travelled by the plume itself [24]. When such data are lacking x_{aggr} is estimated from the observed dependence of x_{aggr} on the laser power density deposited on the target [22], namely

$$x_{aggr} = (t_f\ D')^{1/2}, \tag{6}$$

which is independent of the target, apart from the v_0 value (see eq. (2)). The cluster formation time t_f is the time during which the plume travels the distance x_{aggr}. n_a and n_g are the number densities of ablated and buffer gas atoms, respectively; n_a is given by the ratio between the number of ablated atoms per pulse and the volume of the plume, deduced from fast imaging pictures of the plume. With increasing n_a, the number of collisions between ablated atoms increases, while increasing n_g plume confinement is enhanced. Both mechanisms favour cluster formation and growth. $\sigma_{a\text{-}a}$ and $\sigma_{a\text{-}g}$ are the geometric cross-sections for ablated-particle–ablated-particle and ablated-particle–gas-atom binary collisions. A unit sticking coefficient is taken. Whilst the contribution of elastic collisions to cluster growth is negligible, they play a role to spread the kinetic energy of plume particles; thus both for gas atoms and for ablated species velocity distributions should be considered. The former is a Boltzmann distribution while the latter is non-equilibrium (see the discussion on the choice of v_0 value) at least until the plume becomes non-collisional. Here a further strong simplification is introduced, assuming a single value for both families, namely v_0 for ablated particles and the average velocity v_g for gas atoms, as deduced from gas temperature. The average between v_g and v_0 is taken as the representative average velocity $\langle v \rangle$ of plume particles; it can be considered as the impact velocity in a binary collision between a fast plume particle and a slow buffer gas atom. This choice corresponds to assign a leading role in cluster formation to the fastest ablated particles. When $\langle v \rangle$ increases the time interval between two subsequent collisions decreases, thus enhancing the rate of cluster growth. In both eqs. (5a) and (5b) the first term $(n_a \cdot \sigma_{a\text{-}a} \cdot \langle v \rangle \cdot t_f)$ represents cluster growth and is assumed to be simply proportional to the scattering probability between ablated particles.

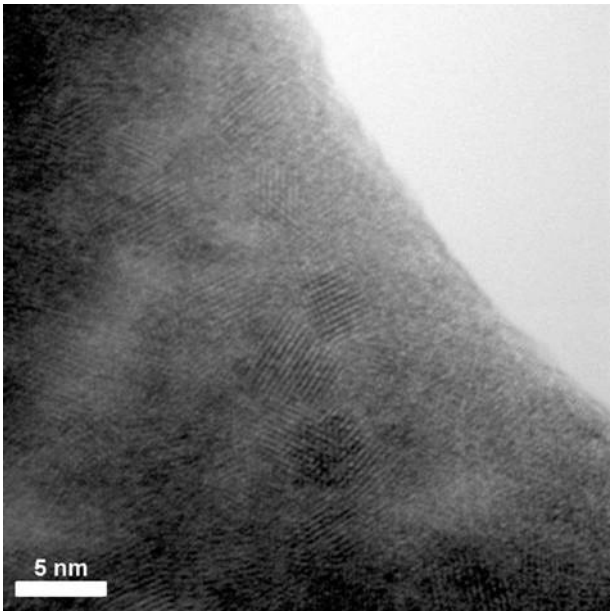

Fig. 3: High-resolution transmission electron microscopy picture from a cluster-assembled tungsten film deposited ablating a W target with laser pulses from a KrF excimer laser ($\lambda = 248\,\text{nm}$, $f = 4.5\,\text{J cm}^{-2}$, $d_{T\text{-}S} = 5\,\text{cm}$) in helium atmosphere ($p_{\text{He}} = 100\,\text{Pa}$). Crystalline clusters (size about 5 nm) embedded in an amorphous matrix are shown.

In both equations the second term $(n_g \cdot \sigma_{a\text{-}g} \cdot \langle v \rangle \cdot t_f)$ mimics plume slowing-down and confinement; it is assumed to be proportional to the scattering probability between ablated particles and gas atoms. In the first plume expansion stage, the dominant mechanism is atom aggregation thereby clusters grow; after the plume has travelled the distance x_{aggr}, cluster growth is *balanced* by cluster cooling both by a leading evaporative and by a less important collisional mechanism.

The competition between growth and cooling mechanisms in a cluster is taken into account by the term $x_{T\text{-}S}x_{aggr}^{-1}$ in eq. (5a) and 1 in eq. (5b). Indeed, this allows avoiding an unphysical indefinitely persisting cluster growth, when the distance flown by the plume were unlimited, as in eq. (5a).

The model of cluster growth was applied to estimate the maximum size of clusters grown in propagating plumes of silicon, tantalum and tungsten. Process conditions and values of model parameters deduced from experiments are collected in table 1 for the above elements.

In the considered experiments $x_{T\text{-}S}$ is larger than x_{aggr}, so that eq. (5b) was used. The number of atoms per cluster is $N_{\text{Si}} = 1.55 \times 10^4$, $N_{\text{Ta}} = 9.6 \times 10^4$, $N_{\text{W1}} = 67$,

N_{W2}= 585, N_{W3}= 5×10^4. For sphere-like clusters, taking a packing efficiency $\eta = 0.67$, typical of close-packed structures, the corresponding average cluster diameters are $d_{Si} = 13.5\,\text{nm}$, $d_{Ta} = 17\,\text{nm}$, $d_{W1} = 1.3\,\text{nm}$, $d_{W2} = 2.7\,\text{nm}$, $d_{W3} = 11.8\,\text{nm}$. Notice the non-linear, strong increase of cluster size with increasing buffer gas pressure.

Notwithstanding the severe approximations involved in the ideal gas model, the calculated cluster diameter values agree with the average size $d = 10\,\text{nm}$ of amorphous silicon clusters, measured by atomic force microscopy [19] and $d = 5$–$10\,\text{nm}$ of crystalline tungsten clusters, observed by transmission electron microscopy in CA films deposited at He pressures from 60 Pa to 200 Pa [30]. As an example, in fig. 3 clusters of about 5 nm diameter observed in a film deposited at $p_{He} = 100\,\text{Pa}$ are shown. A direct comparison is not possible for tantalum clusters due to the lack of data.

Conclusions. – In conclusion, the *mixed-propagation* model allows interpreting and *predicting* the space-time evolution of an ablation plume that propagates in a buffer gas. The results obtained by the model are useful as inputs to calculate, in the frame of the ideal gas approximation, the maximum size of clusters growing *in* the plume during its flight from the target to the substrate. The agreement with available experimental data is good with materials so different from each other as silicon and tungsten are.

* * *

The authors are grateful to G. Radnoczi, Research Institute for Technical Physics and Materials Science, Hungarian Academy of Sciences, Budapest, for transmission electron microscopy observations.

REFERENCES

[1] Boufendi L. *et al.*, *J. Appl. Phys.*, **76** (1994) 148.
[2] Biermann P. and Harwitt M., *Astrophys. J.*, **241** (1980) 105.
[3] Arnas C. *et al.*, *J. Nucl. Mater.*, **353** (2006) 80.
[4] Pushkin M. A. *et al.*, *Appl. Surf. Sci.*, **252** (2006) 4425.
[5] Gupta A., in *Pulsed laser deposition of thin films*, edited by Chrisey D. B. and Hubler G. K. (John Wiley & Sons, New York) 1994, pp. 265–291.
[6] Amoruso S., Toftmann B. and Schou J., *Phys. Rev. E*, **69** (2004) 056403.
[7] Nakata Y., Kalbara H., Okada T. and Maeda M., *J. Appl. Phys.*, **80** (1996) 2458.
[8] Geohegan D. B., in *Pulsed laser deposition of thin films*, edited by Chrisey D. B. and Hubler G. K. (John Wiley & Sons, New York) 1994, pp. 115–165.
[9] Gonzalo J., Afonso C. N. and Madariaga I., *J. Appl. Phys.*, **81** (1997) 951.
[10] Harilal S. S. *et al.*, *J. Appl. Phys.*, **93** (2003) 2380.
[11] Geohegan D. B., *Appl. Phys. Lett.*, **60** (1992) 2732.
[12] Acquaviva S. and De Giorgi M. L., *Appl. Surf. Sci*, **186** (2002) 329.
[13] Rode A. V., Gamaly E. G. and Luther-Davies B., *Appl. Phys. A*, **70** (2000) 135.
[14] Bailini A. and Ossi P. M., *Proc. SPIE*, **6606** (2007) 66060I.
[15] Wood R. F. *et al.*, *Phys. Rev. Lett.*, **79** (1997) 1571.
[16] Arnold N., Gruber J. and Heitz J., *Appl. Phys. A*, **69** (1999) S87.
[17] Bulgakov A. V. and Bulgakova N. M., *J. Phys. D*, **31** (1998) 693.
[18] Gusarov A. V. and Smurov I., *J. Phys. D: Appl. Phys.*, **36** (2003) 2962.
[19] Tillack M. S., Blair D. W. and Harilal S. S., *Nanotechnology*, **15** (2004) 390.
[20] Peterlongo A., Miotello A. and Kelly R., *Phys. Rev. E*, **50** (1994) 4716.
[21] Bailini A. and Ossi P. M., *Appl. Surf. Sci.*, **252** (2006) 4364.
[22] Rivolta A., *Modello per la sintesi di cluster durante deposizione a laser pulsato in gas ambiente*, Laurea Thesis, Politecnico di Milano (2006) (in Italian).
[23] Quarteroni A., *Modellistica Numerica per Problemi Differenziali* (Springer, Milano) 2003, p. 105.
[24] Zhou M. F., Fu Z. W. and Qin Q. Z., *Appl. Surf. Sci*, **125** (1998) 208.
[25] Coey J. M. D., Cole D., Jordan R. and Lunney J. G., *J. Magn. & Magn. Mater.*, **165** (1997) 246.
[26] Amoruso S., Sambri A. and Wang X., *J. Appl. Phys.*, **100** (2006) 013302.
[27] `http://www.webelements.com`, Winter M., Department of Chemistry, University of Sheffield, UK.
[28] Marine W., Patrone L., Luk'yanchuk B. and Sentis M., *Appl. Surf. Sci.*, **154-155** (2000) 345.
[29] Geohegan D. B. and Puretzky A. A., *Appl. Surf. Sci.*, **96-98** (1996) 131.
[30] Di Fonzo F. *et al.*, *Catal. Today*, **116** (2006) 69.